

Influence of boundary conditions on the order and defects of biaxial nematic droplets

C. Chiccoli,¹ L. R. Evangelista,^{2,3,*} P. Pasini,¹ G. Skačej,⁴ R. Teixeira de Souza^{5,6} and C. Zannoni⁶

¹*INFN Sezione di Bologna, Via Irnerio 46, 40126 Bologna, Italy*

²*Departamento de Física, Universidade Estadual de Maringá, Avenida Colombo 5790, 87020-900, Maringá, Paraná, Brazil*

³*Dipartimento di Scienza Applicata del Politecnico di Torino, Corso Duca degli Abruzzi 24, 10129 Torino, Italy*

⁴*Faculty of Mathematics and Physics, University of Ljubljana, Jadranska 19, SI-1000 Ljubljana, Slovenia*

⁵*Departamento Acadêmico de Física, Universidade Tecnológica Federal do Paraná, Campus Apucarana, Rua Marçílio Dias, 635 CEP 86812-460–Apucarana, Paraná, Brazil*

⁶*Dipartimento di Chimica Industriale “Toso Montanari,” Università di Bologna and INSTM, Viale Risorgimento 4, I-40136 Bologna, Italy*



(Received 3 June 2019; published 3 September 2019)

We employ Monte Carlo simulations to study the defects occurring in a nematic droplet formed by biaxial molecules. The simulations are carried out using a lattice model based on a dispersive orientational biaxial potential previously employed to establish the rich phase diagram of the system. The focus of the present investigation is on the molecular organization inside the droplet when bipolar and toroidal anchoring conditions at the surface are considered. In both cases, we describe how the defect structure arises in the system, and we analyze the behavior of the defect core region in connection with the elastic properties of the phase in a continuum theory perspective.

DOI: [10.1103/PhysRevE.100.032702](https://doi.org/10.1103/PhysRevE.100.032702)

I. INTRODUCTION

Nematic droplets formed by biaxial molecules present a rich variety of defects depending on the boundary conditions [1]. To understand these systems is challenging, both from the conceptual as well as the experimental point of view [1–19]. To accomplish the difficult task of describing the defect structure arising in these droplets demands hard theoretical work, and some speculative arguments have continued to be raised in this direction over a few decades [4,15]. In this scenario, computer simulations provide a suitable framework to tackle a whole class of problems in which the biaxiality of the building blocks forming the phases is explicitly taken into account [20]. Recently, we have presented a detailed Monte Carlo study of the effect of molecular biaxiality on the defect created at the center of the nematic droplet in a radial (homeotropic) alignment [21]. Some light has been shed on the important question of the shape and size of the defect core region, already studied in uniaxial nematics [7–13], by showing that the dimensions of the core region may be connected with the biaxiality parameter in the pair potential, at least in the limit of small deformations and low temperature. This connection is demonstrated in the framework of an elastic continuum theory approach, in the limit of weak biaxiality.

In this work, we employ Monte Carlo simulations [22] to perform a study of the formation of the defects in a nematic droplet whose constituents are biaxial molecules, in particular calculating the expected optical textures between cross polarizers. The simulations are carried out using a lattice version [23,24] of the orientational potential for biaxial particles interacting via dispersive forces developed in [20]. We have

already analyzed [21] the case of radial boundary conditions (RBCs), which will be briefly recalled here for completeness. The focus of the present investigation is on the molecular organization inside the droplet when two other important types of planar anchoring at the droplet surface, i.e., bipolar boundary conditions and toroidal boundary conditions, are considered. In all these cases, we show how the defect structure arises in the system, and we analyze the behavior of the defect core region in connection with the elastic properties of the phase and the parameters of the pair potential.

II. MODEL AND SIMULATIONS

To go further, we consider a lattice version of the orientational biaxial potential put forward many years ago by Luckhurst *et al.* [20], and whose phase diagram has already been studied in detail by computer simulations of bulk systems [23,24]. This lattice model, where particle positions are fixed and discretized, only deals with orientational degrees of freedom, thus removing the competition from smectics, but it is able to reproduce the rich phase diagram of a biaxial nematic system in which isotropic, uniaxial, and biaxial phases are present. In addition, it reduces to the well-known Lebwohl-Lasher (LL) uniaxial lattice model for nematics [25], when the molecular biaxiality vanishes. More explicitly, the confined biaxial model Hamiltonian employed in the simulations is written as

$$U_N = \frac{1}{2} \sum_{\substack{i, j \in \mathcal{F} \\ i \neq j}} \Phi_{ij} + J \sum_{\substack{i \in \mathcal{F} \\ j \in \mathcal{S}}} \Phi_{ij}, \quad (1)$$

where \mathcal{F} and \mathcal{S} are the set of particles (let us call them “biaxial spins”) in the bulk and at the surfaces, respectively, i and j are nearest neighbors, while the parameter J models the strength

*lre@dfi.uem.br

of the coupling with the confining surface particles. In this way, the biaxial Hamiltonian is composed of two terms, one of which represents the interaction between the constituent particles (the particles inside the droplet) whereas the other one accounts for the interaction of the mesogenic particles at the surface with those of the surrounding media, i.e., the particles of the host matrix in which the droplet is embedded. The particles interact through the second-rank attractive pair potential:

$$\Phi_{ij} = -\epsilon_{ij} \{ P_2(\cos \beta_{ij}) + 2\lambda [R_{02}^2(\omega_{ij}) + R_{20}^2(\omega_{ij})] + 4\lambda^2 R_{22}^2(\omega_{ij}) \}, \quad (2)$$

where ϵ_{ij} is a positive constant, ϵ , for nearest-neighbor molecules i and j , and zero otherwise; $\omega = \alpha, \beta, \gamma$ is a set of Euler angles [26] and R_{mn}^L are symmetrized combinations of Wigner functions [23]. The biaxiality parameter λ takes into account the deviation from cylindrical molecular symmetry, and, when $\lambda \neq 0$, the particles tend to align not only their major axis, but also their short ones.

We have implemented the alignment at the droplet surface akin to a certain experimental scenario by considering an additional layer of particles kept fixed during the simulation, and with orientation chosen to mimic the desired boundary conditions.

In this framework, as mentioned before, we present a detailed study of biaxial nematic droplets, for various values of molecular biaxiality, with two different boundary conditions, namely bipolar boundary conditions (BBCs)—the long axes are oriented tangentially to the droplet surface and belong to planes parallel to the z axis, and toroidal boundary conditions (TBCs)—the long axes lie in planes perpendicular to the z axis and are oriented tangentially to the droplet surface. In both cases, the short axes of the particles belonging to the surface have random orientations and, as the long axes of the same particles, are frozen during the simulations.

Our model droplets are approximately spherical samples carved from a $50 \times 50 \times 50$ cubic lattice and containing 54 474 particles. We have already verified in previous works that this size, albeit apparently small, is sufficient to simulate with a good resolution the polarized optical microscopy (POM) images observed in experimental work, because a spin can play the role of a packed cluster of tens of molecules instead of a single particle [27]. In the present simulations, the parameter J , denoting the surface coupling with the surrounding environment, was taken equal to 1.

To simulate the optical texture between crossed polarizers, we have employed the Stokes-Müller methodology, considering each spin on the pathway of the incoming photon as a retarder, as in previous work [28,29] and using the following parameters, reported to real units: droplet diameter $d = 5.3 \mu\text{m}$, ordinary and extraordinary refractive indices $n_o = 1.5$ and $n_e = 1.66$, respectively, for a light with wavelength in the visible, and $\lambda_0 = 545 \text{ nm}$ [28,30]. We have also assumed that the refraction tensor can always be considered as effectively uniaxial for the purpose of producing the POM images. The temperature was set to the dimensionless value $T^* = k_B T / \epsilon = 0.1$, deep in the ordered phase. The starting configurations of the lattice were chosen to be completely aligned along the z direction, and the evolution of the system

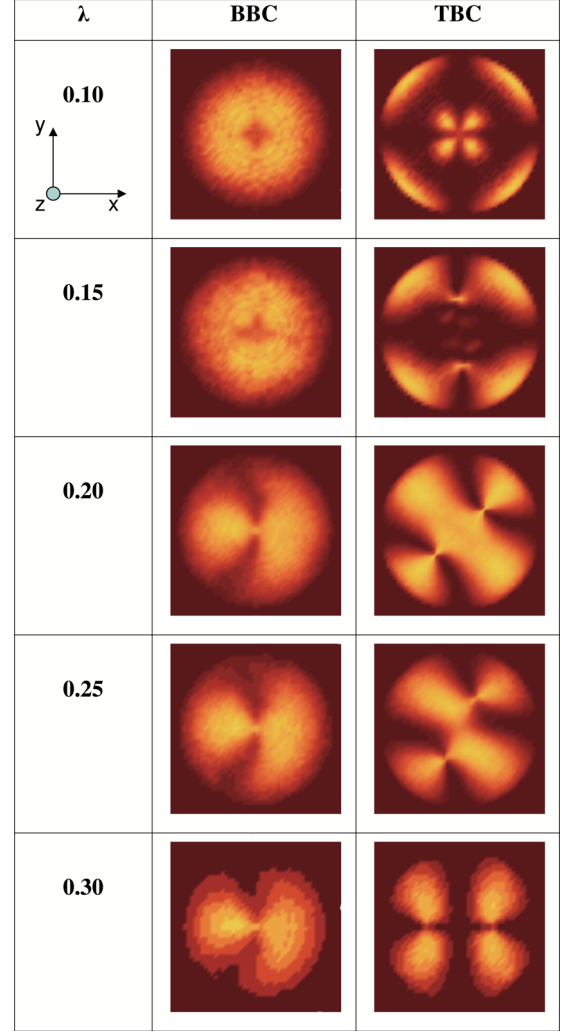


FIG. 1. Top views (from the z axis as shown in the first plate of the first row) of the optical textures obtained from MC simulation of a droplet with different boundary conditions (BBC and TBC) for various values of the molecular biaxiality. The images are simulated between crossed polarizers, and the outgoing light intensity is represented with a false color scale.

was followed according to the classic Metropolis Monte Carlo procedure [22]. The outgoing light intensity is represented with a false color scale to make, at least in principle, comparison with real experiments easier.

III. RESULTS

In Fig. 1, we report the results for the two boundary conditions considered and the dependence of these results on small deviations from the cylindrical symmetry of the constituent molecules of the nematics. We have noticed in a previous work [21] that the main effect for the RBC case is the increasing of the radius of the defect core, placed at the center of the system, which is biaxial itself, as the molecular biaxiality increases. This result was reinforced by a continuum theory analysis relating the biaxiality parameter of the pair potential to the ratio between some elastic constants.

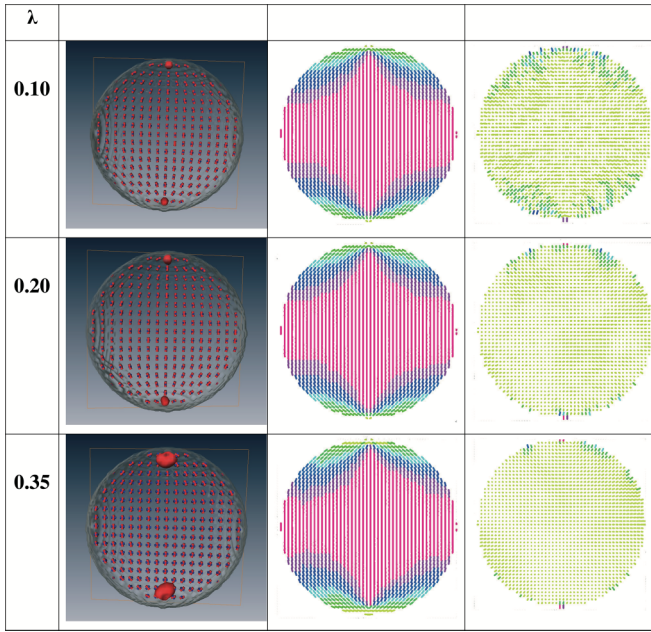


FIG. 2. Plots of the Westin metric isosurfaces for the principal and secondary director (red and blue, respectively) (first column) and vertical cuts of the snapshots of the long (second column) and short (third column) axes for a nematic droplet with BBC alignment and three different values of the biaxiality parameter λ . The isosurface thresholds are chosen in order to provide an optimal visualization of areas where the directors are not well-defined. The color coding of the snapshots varies from red for alignment along z to yellow for an alignment on the xy plane.

Similar observations can now be made also for the BBC case for which two boojums [4] are present at the poles of the droplet, along the z axis in our reference frame. Again, in this case we can appreciate, although smaller with respect to the RBC case, an increasing of the boojums radii as the molecular biaxiality increases (see Fig. 2) by performing a geometric measure for the visualization of second-rank tensor fields and their defects (see, e.g., [31]), and plotting the Westin metric isosurfaces [32] for the principal and secondary director (red and blue, respectively) as reported in Fig. 2. Differently from the RBC case, we have here no appearance of disclination lines for the secondary director as the molecular biaxiality increases. Moreover, we can notice that the area where the principal director is not well-defined, i.e., the size of the defects generated at the poles, seems to slightly increase with the molecular biaxiality (see Fig. 2). These indications given by calculating the Westin metric isosurface are supported by looking carefully at the snapshots of the long axes (second column of Fig. 2).

The case of toroidal boundary conditions (TBCs) seems to be different for what concerns the shape of the defect because there is a change when the deviation from the cylindrical symmetry of the molecules is larger. We can observe the simulated polarized optical textures (Fig. 1) and notice the considerable difference between the results obtained for $\lambda = 0.10$ and those for the higher values of molecular biaxiality. The optical textures are compatible with a point defect for $\lambda = 0.10$ while in the others cases we can observe the appearance

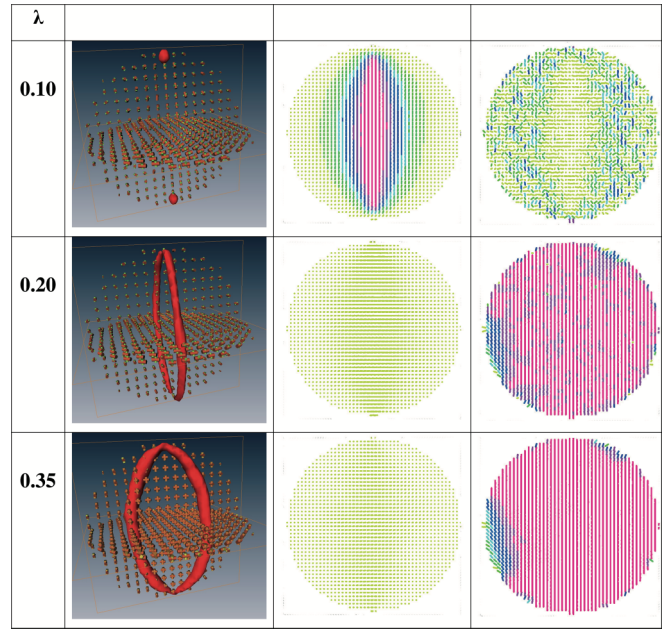


FIG. 3. As in Fig. 2, for the case of toroidal boundary conditions (TBCs).

of two defects. This observation is supported by looking at the calculated Westin isosurfaces reported in Fig. 3, where for the higher values of the molecular biaxiality the shapes of the defects change going from two point defects at the poles of the droplet to a ring defect lying in the plane containing the z axis. To confirm more quantitatively this result, we have calculated the full set [5] of second-rank order parameters. The results are reported in Figs. 4 and 5.

As pointed out by Mermin [4], a configuration that does not give a stable point defect in an ordinary nematic fails to do so in the biaxial nematic. Indeed, as the biaxiality parameter increases, this failure to produce a point defect is evident in Figs. 2 and 3. Even for a small value such as $\lambda = 0.10$, in Fig. 4 one notices the presence of a boojum whose “radius” increases with λ , as illustrated by the conspicuous radius of

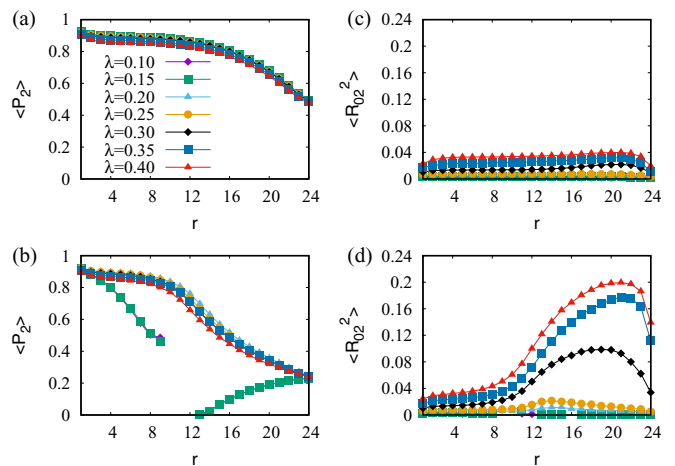


FIG. 4. Second-rank order parameter $\langle P_2 \rangle$ (left column) and $\langle R_{02}^2 \rangle$ (right column) vs distance starting from the center of the droplets for the BBC (top) and TBC (bottom) cases.

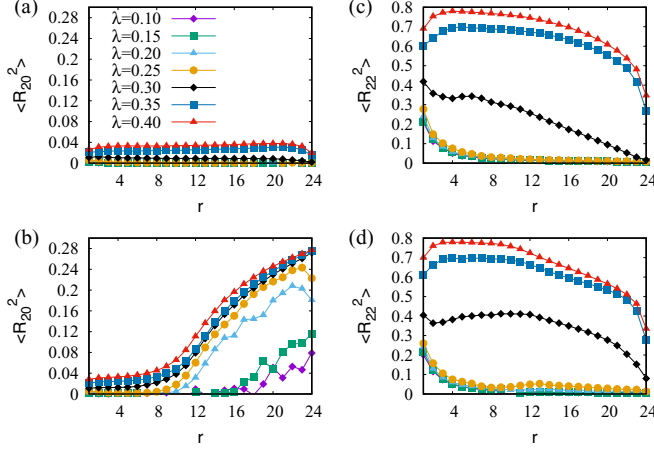


FIG. 5. Second-rank order parameter (R_{20}^2) (first column) and (R_{22}^2) (second column) vs distance starting from the center of the droplets for the BBC (top) and TBC (bottom) cases.

the defect for $\lambda = 0.35$. Similar behavior can be found in Fig. 3 for larger values of λ , thus confirming that the attempt to build a point singularity in a biaxial droplet of nematics gives rise to a line singularity extending outward from the poles, as explicitly shown by the MC simulations.

Furthermore, the fact that the radius of the singularity core increases with the biaxiality parameter λ is expected; it was found also in the case of the droplet under RBC [21] and seems to be mainly connected with the elastic anisotropy, i.e., the rate of growth of the core radius seems to be independent of the boundary conditions employed at least in the cases we considered in the simulation.

To complete the MC investigation, we have calculated the full set of second-rank order parameters across the sample dividing the droplet in concentric shells and computing these observables at every radial distance from the center. The results are reported in Fig. 4, where we show the nematic order parameter $\langle P_2 \rangle$ and the molecular biaxiality parameter $\langle R_{02}^2 \rangle$, and in Fig. 5, which presents the phase biaxiality parameters $\langle R_{20}^2 \rangle$ and $\langle R_{22}^2 \rangle$ for the three different anchoring conditions. Concerning $\langle P_2 \rangle$, we notice a great difference in the behavior for the two cases. For the BBC case, we have a nematic region across the whole system. In the TBC anchoring, we found an inversion in the behavior as λ increases. For what concerns the molecular biaxiality parameter $\langle R_{02}^2 \rangle$, we have also different behavior for the two cases: for BBC, $\langle R_{02}^2 \rangle$ presents no significant variations for the various λ , and, moreover, this parameter is always very small in magnitude across the sample. For TBC, instead, we notice an increasing maximum close to the surfaces as the value of molecular biaxiality parameter increases.

Regarding the phase biaxiality parameters, we notice that $\langle R_{20}^2 \rangle$ exhibits a behavior similar to $\langle R_{02}^2 \rangle$ (see the first row of Fig. 5), and the values of these parameters are always very small. The second phase biaxiality parameter $\langle R_{22}^2 \rangle$ presents higher values than $\langle R_{02}^2 \rangle$, and, for this reason, we have suggested many years ago to monitor this particular parameter to determine the biaxiality [23]. As a matter of fact, also in the present study we notice that we have an ordered biaxial core

at the center of the droplet for all three anchoring conditions, which increases in size with λ .

IV. ELASTIC THEORY

Let us now analyze the role of the molecular biaxiality parameter in an elastic continuum perspective. As we have shown recently [21], the energy of the biaxial nematic, expressed in terms of 12 elastic constants, may be reduced, with a kind of generalized one-elastic constant approximation similar to assuming a one-elastic constant for each axis, to the simplified form [15]

$$f = \frac{1}{2}K_a R_a^2 + \frac{1}{2}K_b R_b^2 + \frac{1}{2}K_c R_c^2, \quad (3)$$

where

$$\begin{aligned} R_a^2 &= (\vec{a} \cdot \nabla \vec{b} \cdot \vec{c})^2 + (\vec{b} \cdot \nabla \vec{b} \cdot \vec{c})^2 + (\vec{c} \cdot \nabla \vec{c} \cdot \vec{b})^2, \\ R_b^2 &= (\vec{b} \cdot \nabla \vec{c} \cdot \vec{a})^2 + (\vec{c} \cdot \nabla \vec{c} \cdot \vec{a})^2 + (\vec{a} \cdot \nabla \vec{a} \cdot \vec{c})^2, \\ R_c^2 &= (\vec{c} \cdot \nabla \vec{a} \cdot \vec{b})^2 + (\vec{a} \cdot \nabla \vec{a} \cdot \vec{b})^2 + (\vec{b} \cdot \nabla \vec{b} \cdot \vec{a})^2, \end{aligned} \quad (4)$$

in which \vec{a} , \vec{b} , and \vec{c} denote the unit vectors specifying the orientation of the biaxial director, with \vec{c} being associated with the longest axis direction. The elastic constants K_a , K_b , and K_c are associated with the deformations in these directions.

In the weak biaxiality approximation, $K_a \approx K_b$, in such a way that $k_{ac} = K_c/K_a$ represents an elastic anisotropy of the nematic phase. On the other hand, λ is the parameter of the potential, Eq. (2), connected with the deviation from uniaxiality of the building blocks, i.e., the bricks representing the molecules. In a pseudomolecular perspective, it is possible to connect the elastic constants characterizing the macroscopic ordering with the anisometric shape of the constituent molecules [33]. By using these well-established features of the elastic parameters and of the molecular ordering, valid in the limit of small deformations and low temperature, it is possible to assume that the relation

$$k_{ac} \propto \lambda^2 \quad (5)$$

holds in general for a biaxial droplet subjected to RBC [21]. Indeed, this can be assumed as an indication that Eq. (5) is a relation connecting the elastic anisotropy with the deviation from uniaxiality of the constituents in a very general way, i.e., it does not depend on the specific surface alignment of the sample because it is also valid in the cases of BBC and TBC. Consequently, since the radius of the defect is surely connected with the elastic anisotropy characteristic of the biaxial phase, the connection stated in Eq. (5) may explain why the radius of the boojum in Fig. 4 and the dimensions of the ring in Fig. 5 also increase with the increasing of the biaxiality parameter. In uniaxial achiral droplets subject to boundary conditions such as those we are dealing with here, such structural changes are induced by parameters such as anchoring energy and elastic constants, in particular the splay and bend ones, as discussed by several authors [34–36]. We can conjecture that such elastic constants can also modify the configurations of defects in biaxial nematic droplets, even if confirming that is in itself a long-term program beyond the scope of this work. Here, even in the case in which the

elastic anisotropy can be negligible, it is remarkable that the molecular organization in these biaxial droplets can also be affected by the intrinsic biaxiality, highlighting the important role of the potential parameter λ and, in particular, its relation with k_{ac} suggested from the elastic theory.

V. CONCLUSIONS

In conclusion, we have explored here how the deviation from the cylindrical symmetry of the constituent molecules influences the formation of the defects in biaxial nematic droplets. In particular, we have analyzed the modification of the defect cores and shapes induced by the different types of boundary conditions for the longest axis of biaxial molecules constituting a nematic liquid crystal droplet. We have focused on two special boundary conditions represented by a bipolar (BBC) and a toroidal (TBC) alignment of the longest axis at the surfaces. The simulations have been carried out by means of a lattice model based on a dispersive potential suitable to tackle biaxial mesogens, which depends on a biaxiality

parameter. The results for bipolar and toroidal boundary conditions reinforce the behavior already found in the case of radial boundary conditions, namely that the core radius increases with the biaxiality parameter, which, in turn, may be connected with the elastic anisotropy of the nematic phase. These results are established in the limit of weak biaxiality and small distortions, keeping the temperature low enough to ensure the applicability of the elastic continuum approach.

ACKNOWLEDGMENTS

L.R.E. and R.T.S. acknowledge financial support from CNPq, Capes and Fundação Araucária (Brazil), and they also thank the INFN–Sezione Bologna (Italy) for partially supporting the visits to Bologna. C.Z. and P.P. thank Oleg Lavrentovich, Kent State University, for useful discussions. C.Z. thanks the Isaac Newton Institute for Mathematical Sciences, Cambridge, UK, for support and hospitality during the program “Mathematical Design of New Materials” when work on this paper was undertaken. This work was supported by EPSRC Grant No. EP/R014604/1.

-
- [1] M. Kleman and O. D. Lavrentovich, *Soft Matter Physics* (Springer-Verlag, New York, 2003).
- [2] P. S. Drzaic, *Liquid Crystal Dispersions* (World Scientific, Singapore, 1995).
- [3] T. Bunning, L. Natarajan, V. Tondiglia, and R. Sutherland, *Annu. Rev. Mater. Sci.* **30**, 83 (2000).
- [4] N. D. Mermin, *Rev. Mod. Phys.* **51**, 591 (1979).
- [5] S. Chandrasekhar and G. Ranganath, *Adv. Phys.* **35**, 507 (1986).
- [6] L. Michel, *Rev. Mod. Phys.* **52**, 617 (1980).
- [7] N. Schopohl and T. J. Sluckin, *J. Phys.* **49**, 1097 (1988).
- [8] E. Penzenstadler and H.-R. Trebin, *J. Phys.* **50**, 1027 (1989).
- [9] H. Mori and H. Nakanishi, *J. Phys. Soc. Jpn.* **57**, 1281 (1988).
- [10] O. D. Lavrentovich and E. M. Terent'ev, *Sov. Phys. JETP* **64**, 1237 (1986).
- [11] C. Chiccoli, P. Pasini, F. Semeria, T. J. Sluckin, and C. Zannoni, *J. Phys. II France* **5**, 427 (1995).
- [12] T. Porenta, M. Ravnik, and S. Žumer, *Soft Matter* **7**, 132 (2011).
- [13] S. Kralj and E. G. Virga, *J. Phys. A* **34**, 829 (2001).
- [14] M. V. Kurik and O. D. Lavrentovich, *Phys. Usp.* **31**, 196 (1988).
- [15] S. Sukumaran and G. Ranganath, *J. Phys. II France* **7**, 583 (1997).
- [16] S. Mkaddem and E. C. Gartland, *Phys. Rev. E* **62**, 6694 (2000).
- [17] M. Kanke and K. Sasaki, *J. Phys. Soc. Jpn.* **82**, 034601 (2013).
- [18] M. Kanke and K. Sasaki, *J. Phys. Soc. Jpn.* **82**, 094605 (2013).
- [19] V. Tomar, S. Hernández, N. Abbott, J. Hernandez-Ortiz, and J. de Pablo, *Soft Matter* **8**, 8679 (2012).
- [20] G. Luckhurst, C. Zannoni, P. Nordio, and U. Segre, *Mol. Phys.* **30**, 1345 (1975).
- [21] C. Chiccoli, L. R. Evangelista, P. Pasini, G. Skačej, R. Teixeira de Souza, and C. Zannoni, *Sci. Rep.* **8**, 2130 (2018).
- [22] M. P. Allen and D. J. Tildesley, *Computer Simulation of Liquids*, 2nd ed. (Oxford University Press, Oxford, 2017).
- [23] F. Biscarini, C. Chiccoli, P. Pasini, F. Semeria, and C. Zannoni, *Phys. Rev. Lett.* **75**, 1803 (1995).
- [24] C. Chiccoli, P. Pasini, F. Semeria, and C. Zannoni, *Int. J. Mod. Phys. C* **10**, 469 (1999).
- [25] P. A. Lebowitz and G. Lasher, *Phys. Rev. A* **6**, 426 (1972).
- [26] M. E. Rose, *Elementary Theory of Angular Momentum* (Wiley, New York, 1957).
- [27] P. Pasini, C. Chiccoli, and C. Zannoni, in *Advances in the Computer Simulations of Liquid Crystals*, edited by P. Pasini and C. Zannoni (Kluwer, Dordrecht, 2000), Vol. 545, pp. 121–138.
- [28] A. Kilian, *Liq. Cryst.* **14**, 1189 (1993).
- [29] R. O. Crawford, E. P. Boyko, B. G. Wagner, J. H. Erdmann, S. Žumer, and J. W. Doane, *J. Appl. Phys.* **69**, 6380 (1991).
- [30] E. Berggren, C. Zannoni, C. Chiccoli, P. Pasini, and F. Semeria, *Phys. Rev. E* **50**, 2929 (1994).
- [31] C.-F. Westin, S. Maier, H. Mamata, A. Nabavi, F. Jolesz, and R. Kikinis, *Med. Image Anal.* **6**, 93 (2002).
- [32] A. C. Callan-Jones, R. A. Pelcovits, V. A. Slavin, S. Zhang, D. H. Laidlaw, and G. B. Lorient, *Phys. Rev. E* **74**, 061701 (2006).
- [33] G. Barbero and L. Evangelista, *An Elementary Course on the Continuum Theory for Nematic Liquid Crystals* (World Scientific, Singapore, 2001).
- [34] G. H. Springer and D. A. Higgins, *J. Am. Chem. Soc.* **122**, 6801 (2000).
- [35] P. Drzaic, *Mol. Cryst. Liq. Cryst. Incorporating Nonlin. Opt.* **154**, 289 (1988).
- [36] J. Jiang and D.-K. Yang, *Liq. Cryst.* **45**, 102 (2018).